Efficient inhibition of SARS-CoV-2 strains by a novel ACE2-IgG4-Fc fusion protein with a stabilized hinge region

Hristo L. Svilenov*[1], Julia Sacherl*[2], Alwin Reiter*[3], Lisa Wolff[2], Cho-Chin Chen[2], Frank-Peter Wachs[3], Susanne Pippig[3], Florian Wolschin[3], Johannes Buchner[1], Carsten Brockmeyer°[3], Ulrike Protzer°[2]

* These authors contributed equally to this work.

° Corresponding authors email: carsten.brockmeyer@formycon.com and protzer@tum.de.

[1] Department of Chemistry, Technische Universität München, Garching, Germany

[2] Institute of Virology, Technische Universität München, Helmholtz Zentrum München, München, Germany

[3] Formycon AG, Martinsried/Planegg, Germany

Abstract

The novel severe acute respiratory syndrome (SARS)-like coronavirus (SARS-CoV-2) enters its host cells after binding the angiotensin-converting enzyme 2 (ACE2) via its spike glycoprotein. This interaction is critical for virus entry and virus-host membrane fusion. Soluble ACE2 ectodomains bind and neutralize the virus but the short *in vivo* half-lives of soluble ACE2 limits its therapeutic use. Fusion of the constant (Fc) part of human immunoglobulin G (IgG) to the ACE2 ectodomain can prolong the *in vivo* half-life but bears the risk of unwanted Fc-receptor activation and antibody-dependent disease enhancement. Here, we describe optimized ACE2-Fc fusion constructs that avoid Fc-receptor binding by using IgG4-Fc as a fusion partner. The engineered ACE2-IgG4-Fc fusion proteins described herein exhibit promising pharmaceutical properties and a broad antiviral activity at single-digit nanomolar concentration. In addition, they allow to maintain beneficial enzymatic activity of ACE2 and thus are very promising candidate antivirals broadly acting against coronaviruses.

Introduction

Of the seven known human pathogenic coronavirus strains, three (SARS-CoV-2, SARS-CoV, NL63) use the angiotensin converting enzyme 2 (ACE2) as the receptor for entry into the human host cell [1-3]. ACE2 is located in the plasma membrane of respiratory epithelial cells [3]. In addition to the respiratory tract, high expression of ACE2 is also found in several other tissues, including intestine, testes, liver, kidney, brain, and cardiovascular system [4-6].

ACE2 is a 805 amino acid type-I transmembrane protein consisting of an extracellular, a transmembrane and a cytosolic domain [7]. The extracellular domain is a zinc metalloprotease, which enzymatically functions as a carboxypeptidase [8, 9] suppressing the renin-angiotensin system (RAS) by cleaving angiotensin I to the inactive angiotensin 1-9 and even more efficiently cleaving angiotensin II to angiotensin 1-7 [10, 11]. Angiotensin 1-7 and its downstream peptides exert a broad spectrum of cell and tissue protection [12], it lowers diastolic blood pressure, has anti-inflammatory, anti-proliferative and anti-fibrotic effects and thereby protects the lung, heart, kidney and other organs from injury [4-6]. The potential contribution of angiotensin II to the COVID-19 pathophysiology has been supported by reports that angiotensin II levels in the plasma samples from COVID-19 patients were markedly elevated and correlated with viral load and severity of disease [13, 14].

ACE2-Fc fusion proteins composed of the human immunoglobulin G (IgG) constant fragment (Fc) fused to the extracellular domain of ACE2 have been suggested as a high-priority treatment option for COVID-19 [15, 16]. In addition to neutralizing SARS-CoV and SARS-CoV-2, the ACE2 enzymatic activity towards the renin-angiotensin system provides a second mode of action, potentially alleviating the acute respiratory distress syndrome (ARDS) pathophysiology. Therapeutic use of a soluble human recombinant ACE2 dimer (APN01) with a half-life of 10 hours is currently investigated in patients with COVID-19 [17-19]. Strong *in vitro* SARS-CoV-2 neutralizing activity has been described for several sequence variants of ACE2-IgG1-Fc fusion proteins [20-25]. A version of an ACE2-IgG1-Fc (HLX71) is in a Phase I clinical study with healthy volunteers [26].

A concern arising from the experience with vaccines and neutralizing antibodies is disease enhancement by Fc effector functions such as complement dependent cytotoxicity (CDC) and antibody dependent cytotoxicity (ADCC) [27]. Moreover, Fc receptor gamma III (CD16) binding, which for example has been shown for neutralizing antibodies in Middle East respiratory syndrome (MERS), has led to infection of CD16 positive cells [28, 29]. It is well known that IgG1-Fc strongly

binds to CD16 and has pronounced CDC and ADCC activity, whereas in contrast for IgG4-Fc such Fc-related effector functions are minimal [30].

For this reason the IgG4 Fc fragment is a preferred fusion partner for ACE2. However, it is well known that naturally occurring IgG4 antibodies are less stable than IgG1 variants due to the formation of half antibodies, which limits their use in pharmaceutical preparations [31-34].

Therefore, we have chosen the immunoglobulin Fc region of an IgG4/kappa isotype with a S228P sequence alteration in the hinge region to stabilize the ACE2-IgG4-Fc fusion protein [32]. For the ACE2 domain two different truncations, Q18-G732 or Q18-S740, respectively, were used for the fusion. In addition, point mutations were introduced in the ACE2 domain to abrogate its enzymatic activity.

Here we report the biophysical and functional characteristic of these ACE2-IgG4-Fc fusion proteins and demonstrate that they efficiently target and entirely neutralize different strains of SARS-CoV-2 as well as SARS-CoV with strain-specific high affinities.

Results

Expression and purification of ACE2-Fc proteins

ACE2-IgG4-Fc and ACE2-IgG1-Fc fusion proteins were designed based on crystal and EM structures of the ACE2 extracellular domain, the SARS-CoV-2 spike protein, and the IgG4-Fc and IgG1-Fc domains [3, 35-37] (**Figure 1 a and b**). Details of the ACE2 sequences fused to the Fc fragments of IgG4 and IgG1 are shown in **Table 1**.

Table 1 Structural properties of the ACE2-Fc constructs

Construct	ACE2 sequence (active site mutation)	IgG isotype (hinge region modification)
1	Q18-G732 (no)	IgG4 (S228P)
2	Q18-S740 (no)	IgG4 (S228P)
3	Q18-G732 (H374N, H378N)	IgG4 (S228P)
4	Q18-S740 (H374N, H378N)	IgG4 (S228P)
5	Q18-G732 (no)	IgG1 (truncated)
6	Q18-S740 (no)	IgG1 (truncated)
7	Q18-G732 (H374N, H378N)	IgG1 (truncated)
8	Q18-S740 (H374N, H378N)	IgG1 (truncated)

Expression yields of all fusion proteins were in a similar range, although slightly higher for Q18-G732 ACE2-Fc fusion proteins. The purity of the ACE2-Fc fusion proteins under investigation was between 95% and 98%, as evident from CE-SDS and SEC analysis. High molecular weight fractions (HMWS) measured after protein A purification were slightly lower for Q18-G732 ACE2-Fc fusion proteins (**Supplementary Table 1**). Peptide mapping confirmed the presence of the modifications in the ACE2-Fc fusion proteins.

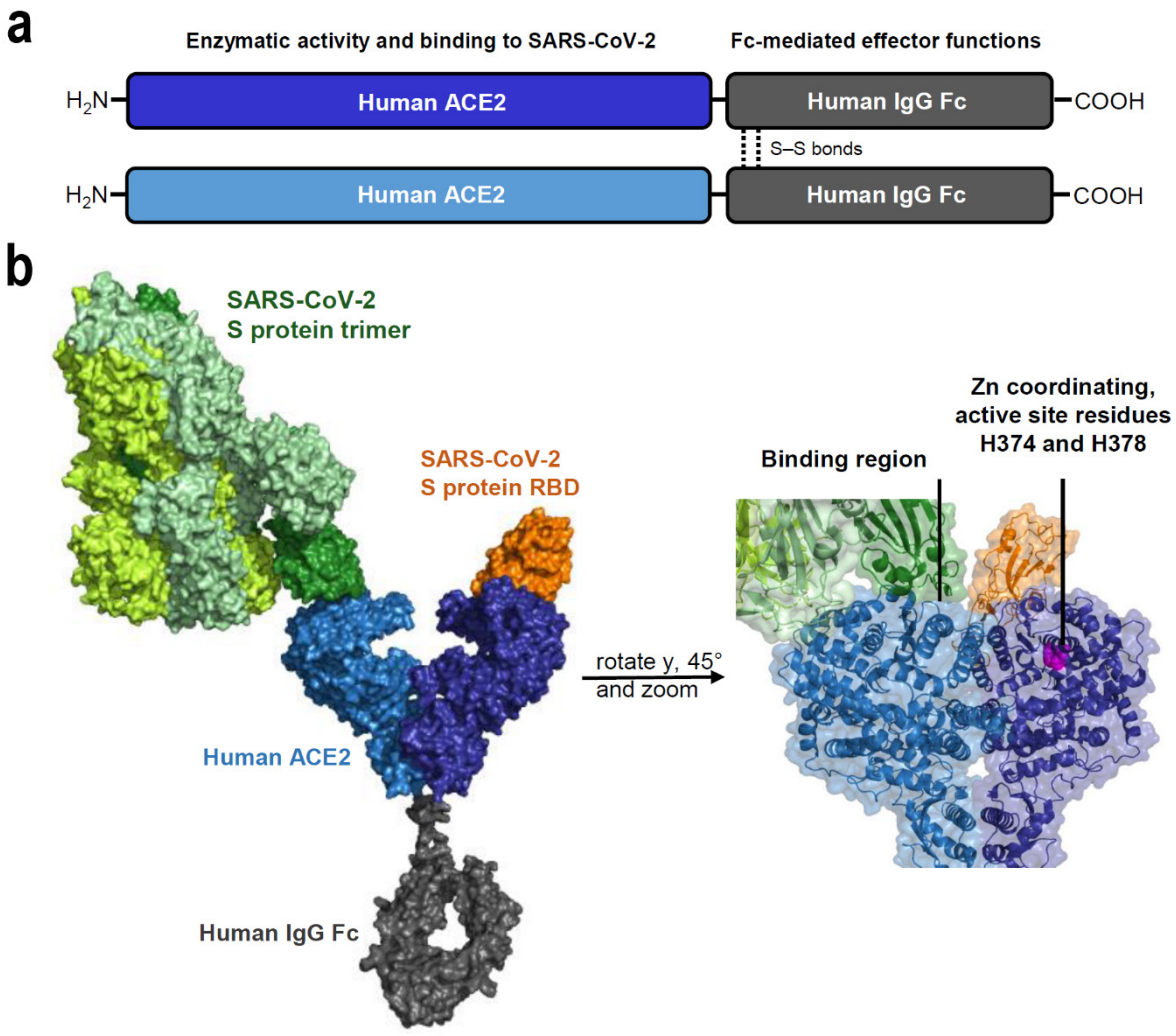

Figure 1 ***Structural elements in the ACE2-Fc constructs. a*** *The main parts in a ACE2-Fc molecule and their functional properties.* ***b*** *ACE2-Fc fusion protein design; ACE2 parts in light and dark blue, IgG-Fc part in gray, Spike protein trimer in green and the RBD of spike protein in orange. The binding region as well as active site residues H374 and H378 important for the enzymatic activity of ACE2 are pointed out in detail. Structures of the following PDB-IDs were used for modeling: 6M17, 6M0J, 6VSB, 5DK3.*

Variations in the ACE2-Fc sequences have a minor effect on the basic structural properties

The Far-UV CD spectra of the fusion proteins are superimposable indicating that the secondary structures are preserved among all constructs, regardless of the sequence variations (**Figure 2a left**). The same is true for the Near-UV CD spectra, which indicate that the overall tertiary structure is also highly similar in all ACE2-Fc proteins investigated (**Figure 2a right**).

Size-exclusion chromatography coupled to multi-angle light scattering (SEC-MALS) was used to investigate the oligomeric state of the fusion proteins. All ACE2-Fc fusion molecules tested exhibit similar elution times and molecular masses of 230 to 235 kDa (**Figure 2b**). These values agree well with the theoretical mass of a homodimer, which is 216-218 kDa based on calculations from the primary sequence. The slightly higher molecular mass measured in solution is due to the glycosylation of the proteins.

Reducing and non-reducing SDS-PAGE (**Figure 2c**) revealed that all ACE2-Fc fusion proteins separated under reduced conditions with DTT run at about 110-120 kDa, which agrees with the theoretical mass for a monomeric ACE2-Fc molecule. The non-reduced ACE2-Fc fusion proteins exhibit a much higher apparent molecular weight, indicating that the intermolecular disulfide bonds in the ACE2-Fc homodimers are formed, which is in agreement with results from CE-SDS under reducing and non-reducing conditions.

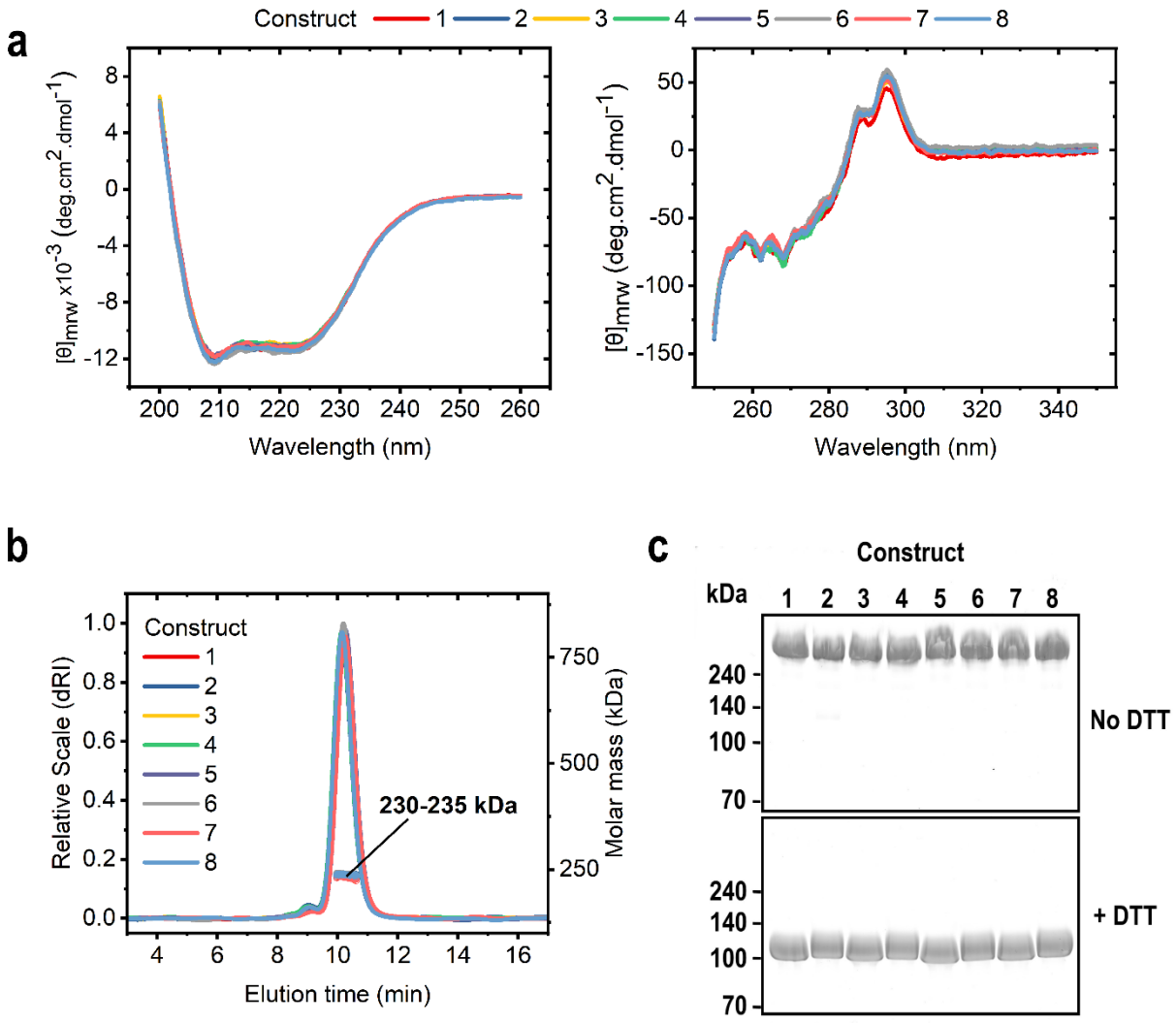

Figure 2 ***Structural characterization of the ACE2-Fc proteins.*** ***a*** *Far-UV CD spectra (left) and Near-UV CD spectra (right) of ACE2-Fc constructs showing that the proteins exhibit same secondary and tertiary structures.* ***b*** *Chromatograms and molecular mass from SEC-MALS indicating that the ACE2-Fc molecules are homodimers.* ***c*** *Non-reducing (top) and reducing (bottom) SDS-PAGE analysis showing that the intermolecular disulfide bonds in the homodimers are formed.*

H374N and H378N mutations abolish enzymatic activity of ACE2-Fc constructs

The *in vitro* assay for the catalytic activity of ACE2 is based on the cleavage of a synthetic peptidyl-MCA derivate and the release of the free MCA fluorophore that has an increased fluorescence intensity at 420 nm (excitation at 320 nm) compared to the peptidyl-MCA. The amount of released MCA was calculated from the slope of the increase in fluorescence intensity and a standard curve with known MCA concentrations. All constructs with wildtype (WT) ACE2 cleave the same amount

of MCA during 30 min of incubation, while the constructs with mutations in the active ACE2 site lost the enzymatic activity (**Figure 3a and b**).

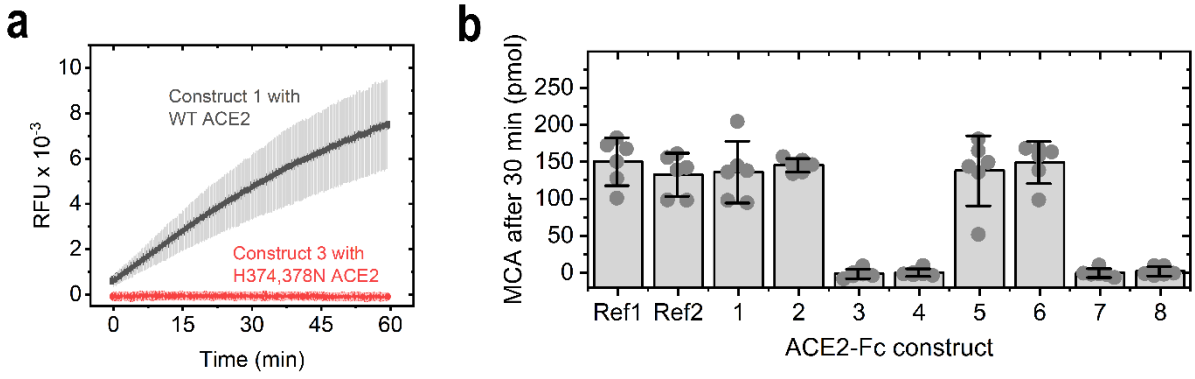

Figure 3 ***Enzymatic activity of the ACE2-Fc constructs. a*** *Comparison of the change in fluorescence signal in the assay for one ACE2-Fc construct with a wildtype ACE2 and one with the H374N and H378N mutations.* ***b*** *Amount of MCA cleaved after 30 min of incubation with the ACE2-Fc constructs. Ref1 and Ref2 are two different commercially available ACE2-Fc proteins from Genscript and Acrobiosystems, respectively. Bars are mean values; error bars depict the 95% confidence interval of six independent experiments.*

Interaction of the ACE2-Fc constructs with the receptor binding domain of SARS-CoV-2

Surface plasmon resonance (SPR) measurements of the ACE2-Fc constructs with the immobilized receptor binding domain (RBD) of SARS-CoV-2 have shown that the ACE2-Fc fusion proteins bind in a concentration-dependent manner to the viral protein, while an unrelated Fc fusion protein (aflibercept) used as a control shows no interaction with the ligand (**Figure 4a**). The derived binding constants demonstrate that all constructs analyzed bind to the immobilized SARS-CoV-2 RBD with a K_D of around 4 nM (**Figure 4b**). This indicates that the structural variations do not influence the interaction between the ACE2-Fc fusion proteins and the RBD of SARS-CoV-2.

Neutralizing activities of the ACE2-Fc fusion proteins against the SARS-CoV-2 spike protein were tested in an inhibitory ELISA. All ACE2-Fc constructs tested bind and potently neutralize the binding of spike S1 protein of SARS-CoV-2 to ACE2 (**Figure 4c**). Consistent with their affinities to the SARS-CoV-2 RBD, there are no significant differences between the different fusion proteins. The half-maximal inhibitory concentrations (IC50 values) for SARS-CoV-2 spike S1 protein neutralization were in the range of 2.5 to 3.5 nM.

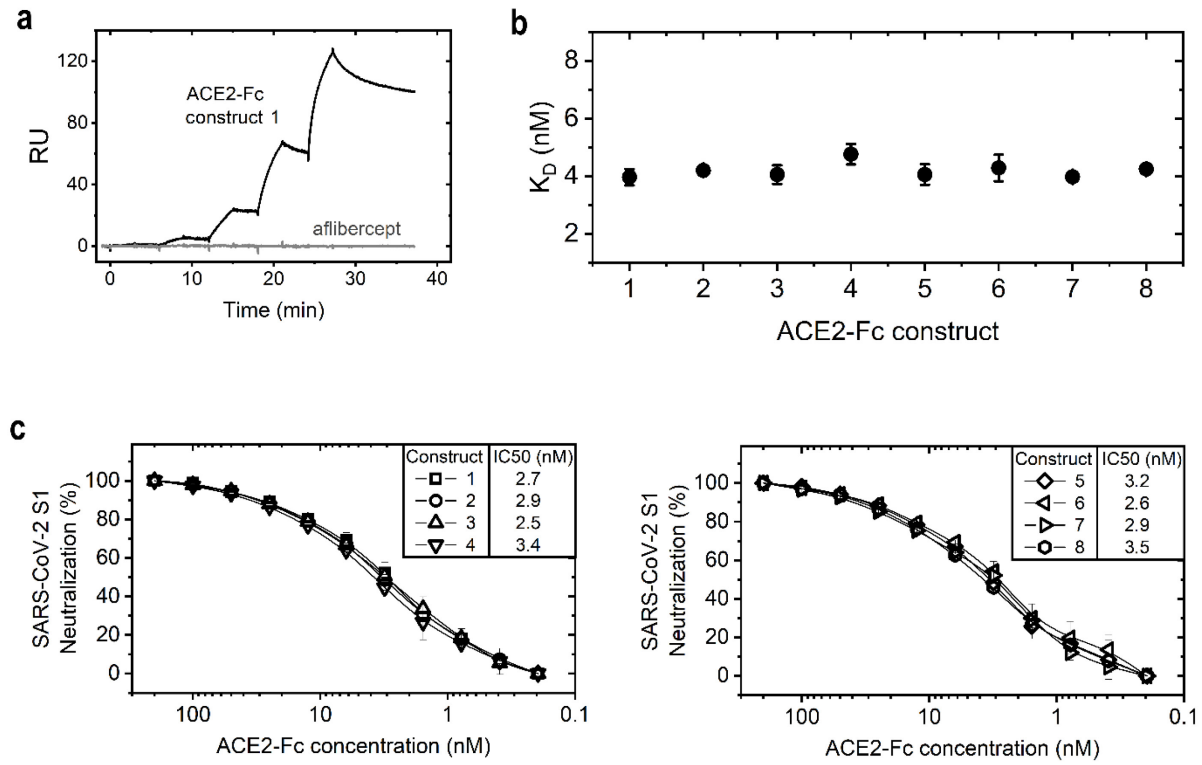

Figure 4 ***Interaction of the ACE2-Fc constructs with the receptor binding domain. a*** *Binding curves of ACE2-Fc molecules to an immobilized RBD from SARS-CoV-2 and an unrelated Fc fusion protein (aflibercept.)* ***b*** *Binding constants of the ACE2-Fc constructs towards the RBD of SARS-CoV-2.* ***c*** *ACE2-Fc fusion proteins were pre-incubated with SARS-CoV-2 spike S1 protein and tested in an ELISA for their ability to neutralize its binding to immobilized ACE2 protein. Potent inhibition of SARS-CoV-2 spike S1 protein by ACE2-IgG4-Fc constructs (left) and ACE2-IgG1-Fc constructs (right). Data are means ± SD of at least two independent experiments.*

Neutralization of SARS-CoV and SARS-CoV-2

All ACE2-IgG-Fc fusion proteins neutralized SARS-CoV (**Figure 5a**) with IC50 values in the range of 150 nM.

When tested for their ability to neutralize SARS-CoV-2, in particular SARS-CoV-2-Jan isolated from a Bavarian COVID-19 patient from the earliest documented COVID-19 outbreak in Germany end of January 2020 [38], all ACE2-Fc fusion proteins displayed strong neutralizing potential against SARS-CoV-2-Jan (**Figure 5b**) with IC50 values in the range of 10 nM.

The ACE2-Fc fusion protein variants were also compared for their ability to neutralize a second SARS-CoV-2 isolate, SARS-CoV-2-April, which was isolated later in the pandemic. The observed plaques of this viral strain showed a different phenotype than SARS-CoV-2-Jan (**Supplementary**

Figure 1). All ACE2-Fc constructs displayed significantly increased neutralizing potential against SARS-CoV-2-April **Figure 5c**) with IC50 values in the range of 1 nM.

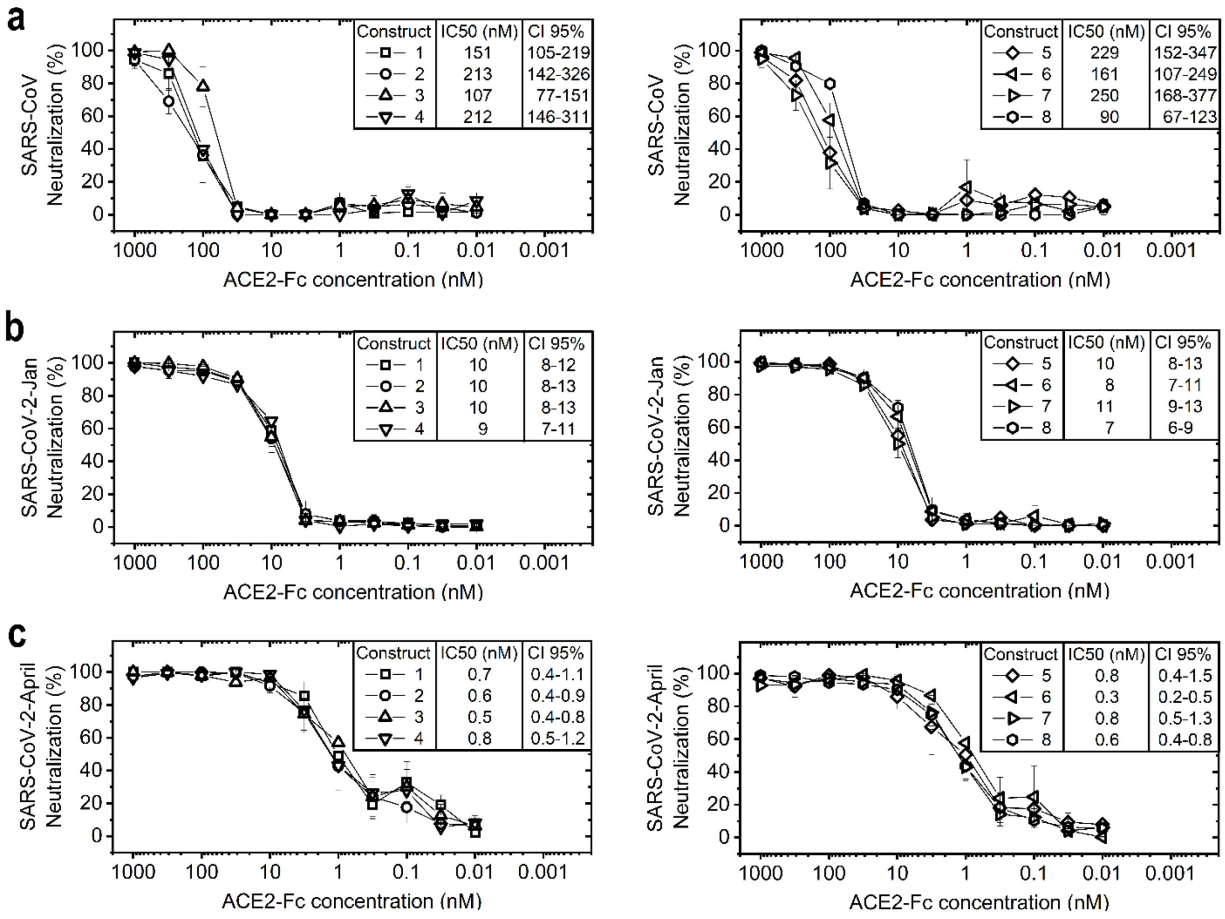

Figure 5 ***ACE2-Fc fusion proteins potently neutralize coronaviruses.*** *ACE2-Fc fusion proteins were pre-incubated with different coronaviruses and tested for their ability to neutralize infection of Vero E6 cells. Potent neutralization of SARS-CoV (**top**), SARS-CoV-2-Jan (**middle**) and SARS-CoV-2-April (**bottom**) by ACE2-IgG4-Fc constructs (**left**) and ACE2-IgG1-Fc constructs (**right**). Data are means ± SEM of three independent experiments.*

Neutralization assay with ACE2-IgG4-Fc using SARS-CoV-2-GFP

The neutralizing capacity of two IgG4 based ACE2-Fc fusion proteins, construct 1 and construct 3, was tested via live cell imaging using the Incucyte S3 platform. Vero E6 cells infected with SARS-CoV-2-GFP pre-incubated with serial dilutions of the two ACE2-IgG4-Fc fusion proteins (ACE2 Q18-G732 wild type and ACE2 Q18-G732 H374N/H378N fused to IgG4-Fc S228P) exhibited concentration dependent complete absence of GFP expression when compared to cells infected

with non-neutralized virus (**Figure 6 and Supplementary Movies**). This shows that Construct 1 and Construct 3 entirely reduce SARS-CoV-2-GFP infection of Vero E6 cells *in vitro*.

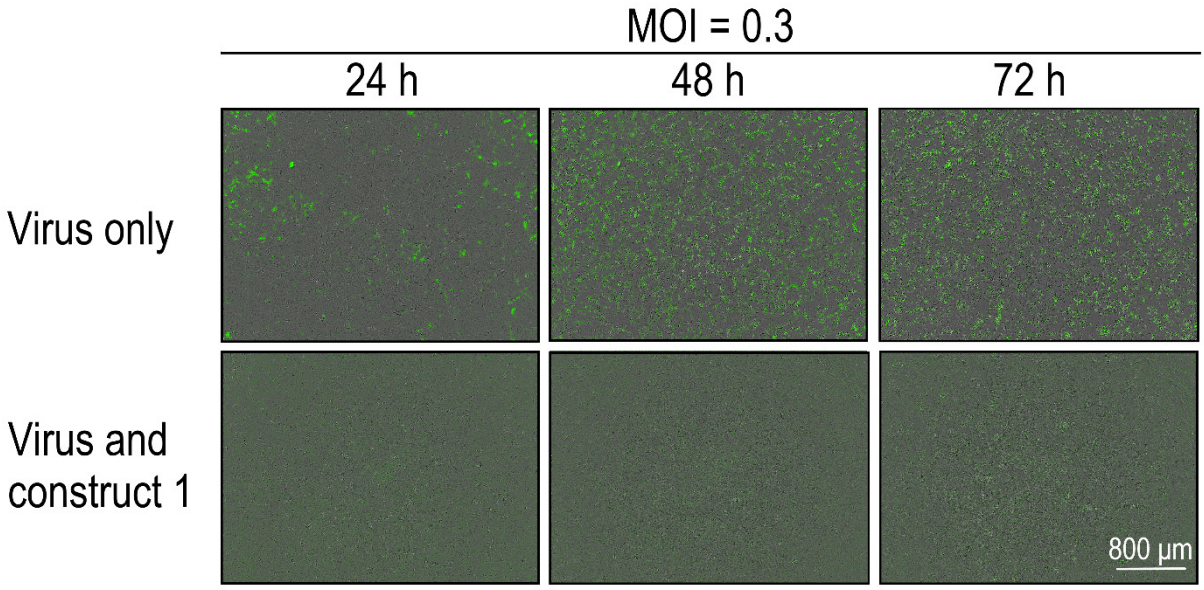

Figure 6 ACE2-IgG-Fc dependent reduction of SARS-CoV-2-GFP replication. *Representative fluorescent images of Vero E6 cells infected with SARS-CoV-2-GFP (Multiplicity of infection (MOI) = 0.3) pre-incubated with ACE2-IgG4-Fc fusion construct 1 (632 nM) (scale bar: 800 µm).*

Discussion

Various sequence variants of ACE2-IgG1-Fc fusion proteins have been described in the literature [20-25]. In this study, novel ACE2-Fc fusion proteins in which the ACE2 domain is fused to the Fc fragment of human immunoglobulin G 4 (ACE2-IgG4-Fc) containing a stabilizing S228P mutation in the hinge region were designed. We used the full length ACE2 ectodomain sequence Q18-S740 and a shortened version comprising Q18-G732. In addition, an ACE2 variant was used comprising two point mutations which abolish its enzymatic activity.

It was thought that ACE2-Fc fusion proteins are homodimers stabilized by disulfide bonds in the hinge region, similar to immunoglobulin G (IgG) [39]. The ACE2 domain and the Fc part likely fold independently, however the Fc domain might have an impact on the overall molecule stability and the interaction with the virus spike protein. We therefore asked whether the Fc fragment isotype impacts expression, purity, and activity of the ACE2 fusion protein.

A comparison of the ACE2-IgG4-Fc and ACE2-IgG1-Fc constructs showed that they express equally well in mammalian cells, suggesting that their *in vivo* folding and assembly efficiency is similar, although yield and purity was slightly higher for the shortened Q18-G732 ACE2 sequence. Also, the enzymatic activity of the ACE2 domain is not affected by the Fc fusion in the wildtype constructs. As expected, the enzymatic activity was completely abolished in the ACE2 point mutants. Thus the basic properties of ACE2 do not seem to be affected in the two different fusion formats. Also the binding to the SARS-CoV-2 viral spike protein as determined by SPR is similar with a K_D of 4 nM. Very similar values were also observed in an ELISA-based SARS-CoV-2 spike S1 protein neutralization for all ACE2-IgG4-Fc and ACE2-IgG1-Fc constructs.

All ACE2-IgG4-Fc and ACE2-IgG1-Fc fusion proteins inhibited Vero E6 cell infection by the SARS-CoV-2 virus isolate SARS-CoV-2-Jan, which was obtained from the earliest documented COVID-19 cases in Germany from January 2020 and is closely related to the original Wuhan strain [38], with IC50 values of around 10 nM. Infection of Vero cells by the predominant SARS-CoV-2-April mutant was inhibited to an even higher degree with IC50 values in the range of 1 nM. In addition, all ACE2-Fc molecules inhibited Vero E6 cell infection by SARS-CoV with IC50 values in the range of 150 nM. These results demonstrate that all ACE2-Fc constructs can effectively neutralize various coronavirus strains.

In line with our results, the affinity of the SARS-CoV-2 spike protein for human ACE2 has been previously reported to be significantly higher than the affinity of the SARS-CoV spike protein [3]. This may explain the high replication rate of SARS-CoV-2 in the upper respiratory tract and thus the high rate of infection.

Investigations on the genome sequences of multiple SARS-CoV-2 isolates reported from various countries identified genomic regions with increased genetic variation [40-42]. Globally, one of these variations, the D614G substitution in the C-terminal region of the spike protein, is now the most prevalent pandemic form [43, 44]. Mutation D614G is associated with an improved ability to bind to ACE2 protein and infection. It has been previously reported that an increase in ACE2 binding affinity makes the SARS-CoV-2 spike protein more sensitive for neutralizing antibodies [45-47]. Here we describe a decrease of the IC50 in the neutralization assays from 10 nM to 1 nM with SARS-CoV-2 isolates obtained from patients in Germany in January 2020 and April 2020 which indicates a further affinity maturation of the SARS-CoV-2 spike protein towards human ACE2 during the course of the pandemic.

ACE2 plays a central role in the homeostatic control of cardio-renal actions and has been shown to protect against severe acute lung injury and acute angiotensin (Ang) II-induced hypertension [48, 49]. Moreover, ACE2 has been identified as a functional receptor for SARS-CoV, SARS-CoV-2 and NL63 [1-3] which is confirmed by our data showing neutralization potency for both SARS-CoV and SARS-CoV-2.

It remains a concern that SARS-CoV-2 and other coronavirus variants have found reservoirs in animals living in close contact with humans and could transmit to humans from time to time, as happened recently with "cluster 5", a SARS-CoV-2 variation with a combination of mutations that is not fully understood for its impact on disease severity and resistance to vaccination and therapeutic antibodies [50, 51]. Compared to vaccines and therapeutic antibodies, which have been associated with a risk of virus escape by mutation as e.g. the occurrence of the spike variant N439K [52-55], administration of ACE2 as a virus blocker provides a high level of protection against drug resistance caused by virus mutation.

Recombinant human ACE2 has therapeutic potential for the SARS-CoV-2 [19, 26]. A soluble dimer (APN019) has been safely tested in a clinical Phase I study in healthy volunteers and in a Phase II study in ARDS patients [17, 18] and is currently being tested for its therapeutic effect in a Phase II study in COVID-19 patients [19].

Pharmacokinetic studies in mice and humans revealed that recombinant human ACE2 exhibits fast clearance rates resulting in a short half-life of only hours [17, 19, 48]. It is well known, that fusing recombinant therapeutic proteins with the Fc region of human immunoglobulin G can result in prolonged plasma half-life of proteins. Therefore, to extend the relatively short plasma half-life of ACE2, the extracellular domain of murine ACE2 has been fused with a murine Fc fragment of immunoglobulin IgG. When tested in murine models of both, acute and chronic models of

angiotensin II-dependent hypertension, murine ACE2-Fc fusion protein demonstrated a prolonged *in vivo* half-life and effective organ protection [56].

The presence of the Fc domain markedly increases the plasma half-life of ACE2-Fc due to the interaction of the Fc domain with the neonatal Fc-receptor (FcRn), and therefore a slower clearance of the fusion molecule. FcRn is broadly expressed on many cell types including endothelial cells and respiratory epithelial cells [57, 58]. Binding to FcRn extends the systemic half-life by chaperoning bound Fc fusion proteins away from lysosomal degradation. In addition, FcRn transports IgG and Fc fusion molecules across mucosal barriers into the lumen of the respiratory and intestinal tract thereby providing a dynamic trafficking between circulating and lumenal IgG molecules at mucosal sites [57, 59]. A human ACE2-Fc fusion protein designed with an IgG1 Fc portion to prolong the circulating half-life is currently in a Phase I clinical study [26].

The affinity of ACE2 dimer to SARS-CoV-2 spike protein is significantly lower compared to ACE2-IgG1-Fc fusion protein [21, 25]. In our study ACE2-IgG4-Fc and ACE2-IgG1-Fc equally have shown high affinity binding to SARS-CoV-2 RBD and spike protein and bound and neutralized various corona virus strains with IC50 values down to 1 nM.

The IgG4 Fc fragment reduces the risk of disease enhancement related to complement dependent cytotoxicity (CDC), antibody dependent cytotoxicity (ADCC) and infection via CD16 Fc receptor [30]. Although the constant heavy chain regions of different IgG subclasses share over 95% sequence homology, their structures and effector functions differ. IgG4 in particular has poor ability to engage C1q and Fc gamma receptors and has been associated with anti-inflammatory properties [60].

The SARS-CoV-2 pandemic has caused an unprecedented challenge to develop COVID-19 drugs in rapid pace. However, progress with candidate therapies has been slow. Here we have shown that ACE2-IgG4-Fc fusion proteins have favorable biophysical and pharmaceutical characteristics and significant *in vitro* neutralizing potency against various corona virus strains. Therefore, ACE2-IgG4-Fc fusion proteins present a promising potential treatment option for the current SARS-CoV-2 pandemic and for future coronavirus infectious diseases.

Material and Methods

Construct design

ACE2 amino acid sequence modifications were designed by computer-aided modelling. ACE2 ectodomains of different length, Q18-G732 and Q18-S740, with or without mutation of the catalytic site (wild type or H374N/H378N mutant) [61] were combined with the Fc fragment of IgG4 bearing a stabilizing S228P mutation in the hinge region [32]. For comparison, the same ACE2 sequence variants were fused to the Fc fragment of IgG1 with a truncated hinge region (DKTHTCPPCPA).

Generation of expression plasmids

Plasmids encoding the Fc fusion proteins were generated at ThermoFisher. Genes of interest were subcloned into pcDNA3.1 Zeocin expression plasmids (Invitrogen V860-20) with a CMV promoter using HindIII/XhoI restriction sites. Following amplification in *Escherichia coli*, expression plasmids were isolated and analyzed by restriction analysis as well as DNA sequencing.

Protein expression

Using the FreeStyle 293 Expression System (ThermoFisher), the different ACE2-Fc fusion proteins were transiently expressed in 3 x 240 mL culture media. On day six, samples were analyzed for cell viability as well as cell density and supernatants were harvested by centrifugation followed by sterile-filtration [62]. The material was either stored at -80°C until purification or subjected directly to purification. Small samples were taken from the pools to determine expression yields by bio-layer interferometry (BLI).

Protein purification

Purification of the fusion proteins secreted into the culture medium was performed by protein A column chromatography followed by preparative Size Exclusion Chromatography (SEC). For protein A purification, after loading the sample, the Amsphere A3 column (JSR Life Sciences) was washed and the ACE2-Fc fusion proteins were eluted using 40 mM NaAc, pH 3.0. Following elution, samples were first neutralized to pH 7.5 using 1 M Tris, pH 9.0, subsequently diluted 1:1 with 50 mM Tris, pH 7.5, 300 mM NaCl and concentrated to 10 mg/mL using spin filters. Concentrated proteins were further purified with a Superdex 200 increase (GE Healthcare) column equilibrated with 50 mM Tris, pH 7.5, 150 mM NaCl. The main peak was pooled, the protein concentration determined by slope spectrometry [63] and adjusted to 1 mg/mL. The protein solution was passed through a sterilizing filter and stored at 4°C until further usage.

Size exclusion chromatography with multi-angle light scattering (SEC-MALS)

A Shimadzu HPLC system with two concentration detectors (UV and refractive index) and a HELEOS II MALS detector were used for the measurements. The flow rate was 1 mL/min and the running buffer was 50 mM Tris, pH 7.5 and 150 mM NaCl. 50 µg of protein was injected on a Superdex 200 Increase 10/300 GL column (Cytiva). The chromatograms were evaluated with the Astra software.

Circular dichroism (CD)

All CD measurements were performed with a Jasco J-1500 spectropolarimeter at 20°C. The sample buffer consisted of 50 mM Tris, pH 7.5 and 150 mM NaCl. The Far-UV CD spectra were obtained in a 1 mm quartz cuvette using a protein concentration of 0.1 mg/mL. The Near-UV CD spectra were measured in a 5 mm quartz cuvette using a protein concentration of 1 mg/mL.

ACE2 activity assay

An ACE2 activity assay kit from Abcam (Cat.No. ab273297) was used to measure the enzymatic activity of the constructs. The assay was performed according to the manufacturer's manual and is based on a methoxycoumarin (MCA) derivative that is cleaved by the ACE2 enzyme. Upon cleavage, free MCA is detected fluorometrically (Ex320nm/Em420nm) and quantified with a standard curve obtained with MCA standard solutions with known concentrations. Two commercially available ACE2-Fc proteins obtained from Genscript (Cat.No. Z03484-1) and Acrobiosystems (Cat.No. AC2-H5257) were used as reference.

Determination of binding affinity to spike protein RBD using surface plasmon resonance (SPR)

The measurements were performed with a Biacore X-100 system and the Biotin CAPture kit (Cytiva). The running buffer was HBS-EB+ (Cytiva). The ligand, SARS-CoV-2 RBD with an AviTag (Acrobiosystems) was immobilized on the streptavidin chip to around 100 RU. Increasing concentrations of the analyte ACE2-Fc (0.32, 1.6, 8, 40 and 200 nM) were injected over the immobilized ligand in a single-cycle kinetic mode. The obtained sensorgrams were evaluated with the Biacore X-100 software to obtain a binding constant (K_D).

SARS-CoV-2 Spike S1 Inhibition ELISA

Inhibition of binding of SARS-CoV-2 spike S1 protein to ACE2 was tested using the ACE2:SARS-CoV-2 Spike S1 Inhibitor Screening Assay Kit (BPS Bioscience; Cat.No. 79945) according to the manufacturer's instructions with an adapted neutralization procedure. Briefly, biotinylated SARS-CoV-2 Spike S1 protein (25 nM) was incubated with serial dilutions of the ACE2-Fc fusion proteins

in a 96-well neutralization plate at room temperature (RT) for one hour with slow shaking (= neutralization mix).

ACE2 protein was added to a nickel-coated 96-well plate at a concentration of 1 µg/mL and incubated at RT for one hour with slow shaking. Following a washing step to remove unbound ACE2, the plates were blocked for 10 min at RT with slow shaking. Subsequently, the neutralization mix was transferred to the ACE2 coated plate and the plate was incubated at RT for one hour with slow shaking. Following a 10 min blocking step, the plate was incubated for one hour at RT with slow shaking with Streptavidin-HRP. Following a washing and a 10 min blocking step, the HRP substrate was added and the plate was analyzed on a chemiluminescence reader.

Virus strains

SARS-CoV-2-Jan (SARS-CoV-2-Munich-TUM-1; EPI_ISL_582134), SARS-CoV-2-April (SARS-CoV-2 D614G; EPI_ISL_466888), and SARS-CoV (AY291315.1) were isolated from patient material in Germany. Briefly, SARS-CoV-2-Jan was isolated from a Bavarian COVID-19 patient from the earliest documented COVID-19 outbreak in Germany at end of January 2020 which originated from Wuhan [64]. SARS-CoV-2-April was isolated later in the pandemic (April 2020) from a patient in Munich.

SARS-CoV-2-Jan, SARS-CoV and SARS-CoV-2-GFP [65] were propagated and passaged in Vero E6 cells (derived from African green monkey kidney epithelial cells). SARS-CoV-2-April was propagated by the infection of Caco-2 cells followed by passaging in Vero E6 cells. All strains were cultured in DMEM medium (5% fetal calf serum (FCS), 1% penicillin/streptomycin (P/S), 200 mmol/L L-glutamine, 1% MEM-non-essential amino acids, 1% sodium-pyruvate (all from Gibco). Viral titer was determined by Plaque Assay.

Plaque Assay

Viral titers were determined as described by Baer et al., [64] with some modifications. Briefly, HepG2 or Vero E6 cells were plated in a 12-well plate at 5 x 10E5 cells/well in DMEM medium (Gibco) supplemented with 5% FCS, 1% P/S, 200 mmol/L L-glutamine, 1% MEM-non-essential amino acids, 1% sodium-pyruvate (all from Gibco) and incubated overnight at 37°C and 5% CO_2. Cells were infected with serial dilution of virus sample in cell culture medium at 37°C for one hour. After discarding the supernatant, 1 mL of 5% carboxymethylcellulose (Sigma) diluted in Minimum Essential Media (Gibco) was added per well and the plate was incubated at 37°C until obvious plaques appeared. After removing the supernatant, cells were fixed with 10% paraformaldehyde (ChemCruz) for 30 min at RT. Next, a washing step with PBS was performed, followed by the

addition of 1% crystal violet (Sigma; diluted in 20% methanol and water). Following an incubation time of 15 min at RT, the solution was washed away with PBS and the plate was dried. The viral titer (PFU/mL) of the sample was determined by counting the average number of plaques for a dilution and the inverse of the total dilution factor.

SARS-CoV-2 virus neutralization assay

Viral neutralization assay followed by in-cell ELISA

Vero E6 cells were plated in a 96-well plate at 1.6 x 10E04 cells/well in DMEM medium (Gibco) supplemented with 5% FCS, 1% penicillin-streptomycin, 200 mmol/L L-glumatine, 1% MEM-non-essential amino acids, 1% sodium-pyruvate (all from Gibco) and incubated overnight at 37°C and 5% CO_2. Serial dilutions of the ACE2-Fc fusion proteins were mixed with virus in fresh media and pre-incubated for one hour at 37°C. The Vero E6 cells were infected at a multiplicity of infection (MOI) of 0.03 with the neutralized virus solution for one hour at 37°C. Next, the neutralization mix was removed, culture medium was added, and cells were incubated at 37°C for 24 hours. Mock cells represent uninfected Vero E6 cells, incubated with culture medium. After 24 hours cells were washed once with PBS and fixed with 4% paraformaldehyde (ChemCruz) for 10 min at RT. Following a washing step with PBS, fixed Vero E6 cells were permeabilized with 0.5% saponin (Roth) in PBS for 10 min at RT. Next, the permeabilization solution was removed and cells were blocked with a mixture of 0.1% saponin and 10% goat serum (Sigma) in PBS with gentle shaking at RT for one hour. Subsequently, Vero E6 cells were incubated with a 1:500 dilution of an anti-dsRNA J2 antibody (Jena Bioscience) in PBS supplemented with 1% FCS at 4°C overnight with shaking. Following four washing steps with wash buffer (PBS supplemented with 0.05% Tween-20 (Roth)). Next, the plates were incubated with a 1:2,000 dilution of a goat anti-mouse IgG2a-HRP antibody (Southern Biotech) in PBS supplemented with 1% FCS and incubated with gently shaking at RT for one hour. Following four washing steps, 3,3′,5,5′-Tetramethylbenzidin (TMB) substrate (Invitrogen) was added to the wells and incubated in the dark for 10 min. Colorimetric detection on a Tecan infinite F200 pro plate reader at 450 nm and at 560 nm was performed after stopping the color reaction by the addition of 2N H_2SO_4 (Roth).

Viral neutralization assay using SARS-CoV-2-GFP

Vero E6 cells were plated in a 96-well plate at 1.4 x 10E04 cells/well in DMEM medium (Gibco) supplemented with 5% FCS, 1% P/S, 200 mmol/L L-glumatine, 1% MEM-non-essential amino acids, 1% sodium-pyruvate (all from Gibco) and incubated overnight at 37°C and 5% CO_2. Serial dilutions of ACE2-Fc fusion proteins and SARS-CoV-2-GFP were mixed in fresh media and pre-incubated for one hour at 37°C. Vero E6 cells were infected at an MOI of 0.3 with the neutralized

virus solution for one hour at 37°C. Afterwards, the neutralization mix was replaced by cell culture medium. Plates were placed in the IncuCyte S3 Live-Cell Analysis System and real-time images of uninfected mock cells (Phase channel) and infected (GFP and Phase channel) cells were captured every four hours for 72 hours. Virus control cells were infected only with virus.

Acknowledgements:

The authors like to thank Polpharma Biologics Utrecht B.V. for performing the transient transfections and providing the fusion molecules.

Supported by grant AZ-1433-20 of the Bayerische Forschungsstiftung.

References

1. Hofmann, H., et al., *Human coronavirus NL63 employs the severe acute respiratory syndrome coronavirus receptor for cellular entry.* Proc Natl Acad Sci U S A, 2005. **102**(22): p. 7988-93.
2. Hoffmann, M., et al., *SARS-CoV-2 Cell Entry Depends on ACE2 and TMPRSS2 and Is Blocked by a Clinically Proven Protease Inhibitor.* Cell, 2020. **181**(2): p. 271-280 e8.
3. Wrapp, D., et al., *Cryo-EM structure of the 2019-nCoV spike in the prefusion conformation.* Science, 2020. **367**(6483): p. 1260-1263.
4. Crackower, M.A., et al., *Angiotensin-converting enzyme 2 is an essential regulator of heart function.* Nature, 2002. **417**(6891): p. 822-8.
5. Ding, Y., et al., *Organ distribution of severe acute respiratory syndrome (SARS) associated coronavirus (SARS-CoV) in SARS patients: implications for pathogenesis and virus transmission pathways.* J Pathol, 2004. **203**(2): p. 622-30.
6. Hamming, I., et al., *Tissue distribution of ACE2 protein, the functional receptor for SARS coronavirus. A first step in understanding SARS pathogenesis.* J Pathol, 2004. **203**(2): p. 631-7.
7. Jiang, F., et al., *Angiotensin-converting enzyme 2 and angiotensin 1-7: novel therapeutic targets.* Nat Rev Cardiol, 2014. **11**(7): p. 413-26.
8. Donoghue, M., et al., *A novel angiotensin-converting enzyme-related carboxypeptidase (ACE2) converts angiotensin I to angiotensin 1-9.* Circ Res, 2000. **87**(5): p. E1-9.
9. Tipnis, S.R., et al., *A human homolog of angiotensin-converting enzyme. Cloning and functional expression as a captopril-insensitive carboxypeptidase.* J Biol Chem, 2000. **275**(43): p. 33238-43.
10. Lu, H., et al., *Structure and functions of angiotensinogen.* Hypertens Res, 2016. **39**(7): p. 492-500.
11. Santos, R.A.S., et al., *The ACE2/Angiotensin-(1-7)/MAS Axis of the Renin-Angiotensin System: Focus on Angiotensin-(1-7).* Physiol Rev, 2018. **98**(1): p. 505-553.
12. Burrell, L.M., et al., *ACE2, a new regulator of the renin-angiotensin system.* Trends Endocrinol Metab, 2004. **15**(4): p. 166-9.
13. Liu, M.Y., et al., *Role and mechanism of angiotensin-converting enzyme 2 in acute lung injury in coronavirus disease 2019.* Chronic Dis Transl Med, 2020. **6**(2): p. 98-105.
14. Wu, J., et al., *Advances in research on ACE2 as a receptor for 2019-nCoV.* Cell Mol Life Sci, 2020.
15. Kruse, R.L., *Therapeutic strategies in an outbreak scenario to treat the novel coronavirus originating in Wuhan, China.* F1000Res, 2020. **9**: p. 72.
16. Batlle, D., J. Wysocki, and K. Satchell, *Soluble angiotensin-converting enzyme 2: a potential approach for coronavirus infection therapy?* Clin Sci (Lond), 2020. **134**(5): p. 543-545.
17. Haschke, M., et al., *Pharmacokinetics and pharmacodynamics of recombinant human angiotensin-converting enzyme 2 in healthy human subjects.* Clin Pharmacokinet, 2013. **52**(9): p. 783-92.
18. Khan, A., et al., *A pilot clinical trial of recombinant human angiotensin-converting enzyme 2 in acute respiratory distress syndrome.* Crit Care, 2017. **21**(1): p. 234.
19. Zoufaly, A., et al., *Human recombinant soluble ACE2 in severe COVID-19.* The Lancet Respiratory Medicine, 2020.
20. Liu, P., et al., *Designed variants of ACE2-Fc that decouple anti-SARS-CoV-2 activities from unwanted cardiovascular effects.* Int J Biol Macromol, 2020. **165**(Pt B): p. 1626-1633.
21. Iwanaga, N., et al., *Novel ACE2-IgG1 fusions with improved activity against SARS-CoV2.* bioRxiv, 2020: p. 2020.06.15.152157.

22. Huang, K.Y., et al., *Humanized COVID-19 decoy antibody effectively blocks viral entry and prevents SARS-CoV-2 infection.* EMBO Mol Med, 2020. **n/a**(n/a): p. e12828.
23. Lui, I., et al., *Trimeric SARS-CoV-2 Spike interacts with dimeric ACE2 with limited intra-Spike avidity.* bioRxiv, 2020: p. 2020.05.21.109157.
24. Lei, C., et al., *Neutralization of SARS-CoV-2 spike pseudotyped virus by recombinant ACE2-Ig.* Nat Commun, 2020. **11**(1): p. 2070.
25. Glasgow, A., et al., *Engineered ACE2 receptor traps potently neutralize SARS-CoV-2.* Proc Natl Acad Sci U S A, 2020.
26. Hengenix Biotech Inc., *Evaluate the Safety, Tolerability, Pharmacodynamics, Pharmacokinetics, and Immunogenicity of HLX71 (Recombinant Human Angiotensin-converting Enzyme 2-Fc Fusion Protein for COVID-19) in Healthy Adult Subjects*. 2020.
27. Bournazos, S., A. Gupta, and J.V. Ravetch, *The role of IgG Fc receptors in antibody-dependent enhancement.* Nat Rev Immunol, 2020. **20**(10): p. 633-643.
28. Jafarzadeh, A., et al., *Contribution of monocytes and macrophages to the local tissue inflammation and cytokine storm in COVID-19: Lessons from SARS and MERS, and potential therapeutic interventions.* Life Sci, 2020. **257**: p. 118102.
29. Manickam, C., S. Sugawara, and R.K. Reeves, *Friends or foes? The knowns and unknowns of natural killer cell biology in COVID-19 and other coronaviruses in July 2020.* PLoS Pathog, 2020. **16**(8): p. e1008820.
30. de Taeye, S.W., et al., *FcgammaR Binding and ADCC Activity of Human IgG Allotypes.* Front Immunol, 2020. **11**(740): p. 740.
31. Correia, I.R., *Stability of IgG isotypes in serum.* MAbs, 2010. **2**(3): p. 221-32.
32. Aalberse, R.C. and J. Schuurman, *IgG4 breaking the rules.* Immunology, 2002. **105**(1): p. 9-19.
33. Dumet, C., et al., *Insights into the IgG heavy chain engineering patent landscape as applied to IgG4 antibody development.* MAbs, 2019. **11**(8): p. 1341-1350.
34. Handlogten, M.W., et al., *Prevention of Fab-arm exchange and antibody reduction via stabilization of the IgG4 hinge region.* MAbs, 2020. **12**(1): p. 1779974.
35. Yan, R., et al., *Structural basis for the recognition of SARS-CoV-2 by full-length human ACE2.* Science, 2020. **367**(6485): p. 1444-1448.
36. Lan, J., et al., *Structure of the SARS-CoV-2 spike receptor-binding domain bound to the ACE2 receptor.* Nature, 2020. **581**(7807): p. 215-220.
37. Scapin, G., et al., *Structure of full-length human anti-PD1 therapeutic IgG4 antibody pembrolizumab.* Nat Struct Mol Biol, 2015. **22**(12): p. 953-8.
38. Bohmer, M.M., et al., *Investigation of a COVID-19 outbreak in Germany resulting from a single travel-associated primary case: a case series.* Lancet Infect Dis, 2020. **20**(8): p. 920-928.
39. Bernardi, A., et al., *Development and simulation of fully glycosylated molecular models of ACE2-Fc fusion proteins and their interaction with the SARS-CoV-2 spike protein binding domain.* PLoS One, 2020. **15**(8): p. e0237295.
40. Khan, M.I., et al., *Comparative genome analysis of novel coronavirus (SARS-CoV-2) from different geographical locations and the effect of mutations on major target proteins: An in silico insight.* PLoS One, 2020. **15**(9): p. e0238344.
41. Islam, M.R., et al., *Genome-wide analysis of SARS-CoV-2 virus strains circulating worldwide implicates heterogeneity.* Sci Rep, 2020. **10**(1): p. 14004.
42. Mercatelli, D. and F.M. Giorgi, *Geographic and Genomic Distribution of SARS-CoV-2 Mutations.* Front Microbiol, 2020. **11**(1800): p. 1800.
43. Korber, B., et al., *Tracking Changes in SARS-CoV-2 Spike: Evidence that D614G Increases Infectivity of the COVID-19 Virus.* Cell, 2020. **182**(4): p. 812-827 e19.
44. Fernandez, A., *Structural Impact of Mutation D614G in SARS-CoV-2 Spike Protein: Enhanced Infectivity and Therapeutic Opportunity.* ACS Med Chem Lett, 2020. **11**(9): p. 1667-1670.

45. Plante, J.A., et al., *Spike mutation D614G alters SARS-CoV-2 fitness.* Nature, 2020.
46. Weissman, D., et al., *D614G Spike Mutation Increases SARS CoV-2 Susceptibility to Neutralization.* medRxiv, 2020: p. 2020.07.22.20159905.
47. Zhang, L., et al., *The D614G mutation in the SARS-CoV-2 spike protein reduces S1 shedding and increases infectivity.* bioRxiv, 2020: p. 2020.06.12.148726.
48. Wysocki, J., et al., *Targeting the degradation of angiotensin II with recombinant angiotensin-converting enzyme 2: prevention of angiotensin II-dependent hypertension.* Hypertension, 2010. **55**(1): p. 90-8.
49. Tikellis, C. and M.C. Thomas, *Angiotensin-Converting Enzyme 2 (ACE2) Is a Key Modulator of the Renin Angiotensin System in Health and Disease.* Int J Pept, 2012. **2012**: p. 256294.
50. Mallapaty, S., *COVID mink analysis shows mutations are not dangerous - yet.* Nature, 2020. **587**(7834): p. 340-341.
51. Oude Munnink, B.B., et al., *Transmission of SARS-CoV-2 on mink farms between humans and mink and back to humans.* Science, 2020: p. eabe5901.
52. Zimmermann, P. and N. Curtis, *Factors That Influence the Immune Response to Vaccination.* Clin Microbiol Rev, 2019. **32**(2): p. e00084-18.
53. Florindo, H.F., et al., *Immune-mediated approaches against COVID-19.* Nat Nanotechnol, 2020. **15**(8): p. 630-645.
54. Jeyanathan, M., et al., *Immunological considerations for COVID-19 vaccine strategies.* Nat Rev Immunol, 2020. **20**(10): p. 615-632.
55. Thomson, E.C., et al., *The circulating SARS-CoV-2 spike variant N439K maintains fitness while evading antibody-mediated immunity.* bioRxiv, 2020: p. 2020.11.04.355842.
56. Liu, P., et al., *Novel ACE2-Fc chimeric fusion provides long-lasting hypertension control and organ protection in mouse models of systemic renin angiotensin system activation.* Kidney Int, 2018. **94**(1): p. 114-125.
57. Sockolosky, J.T. and F.C. Szoka, *The neonatal Fc receptor, FcRn, as a target for drug delivery and therapy.* Adv Drug Deliv Rev, 2015. **91**: p. 109-24.
58. Latvala, S., et al., *Distribution of FcRn Across Species and Tissues.* J Histochem Cytochem, 2017. **65**(6): p. 321-333.
59. Tzaban, S., et al., *The recycling and transcytotic pathways for IgG transport by FcRn are distinct and display an inherent polarity.* J Cell Biol, 2009. **185**(4): p. 673-84.
60. Muhammed, Y., *Best IgG Subclass for the Development of Therapeutics Monoclonal Antibodies Drugs and their Commercial Production: A Review.* Immunome Res, 2020. **16**(1).
61. Moore, M.J., et al., *Retroviruses pseudotyped with the severe acute respiratory syndrome coronavirus spike protein efficiently infect cells expressing angiotensin-converting enzyme 2.* J Virol, 2004. **78**(19): p. 10628-35.
62. Walls, A.C., et al., *Structure, Function, and Antigenicity of the SARS-CoV-2 Spike Glycoprotein.* Cell, 2020. **181**(2): p. 281-292 e6.
63. Lehr, B., et al., *Evaluation of a Variable-Pathlength Spectrophotometer: A Comparable Instrument for Determining Protein Concentration.* BioProcess International, 2015. **13**(6): p. 46-51.
64. Baer, A. and K. Kehn-Hall, *Viral concentration determination through plaque assays: using traditional and novel overlay systems.* J Vis Exp, 2014(93): p. e52065.
65. Thi Nhu Thao, T., et al., *Rapid reconstruction of SARS-CoV-2 using a synthetic genomics platform.* Nature, 2020. **582**(7813): p. 561-565.

Supplementary Material and Methods

Analytical SEC

Purified proteins were analyzed by analytical Size Exclusion Chromatography (SEC) on a Waters H-Class bio UPLC system using an Acquity UPLC Protein BEH SEC column, 4.6 mm x 150mm, 200Å, 1.7 µm. Detection was based on UV absorbance at 280 nm. 20 µg of samples were loaded, the mobile phase consisted of 20 mM sodium phosphate pH 7.0, 150 mM NaCl and proteins were eluted isocratically at a flow rate of 0.3 mL/min.

Capillary Electrophoresis - Sodium Dodecyl Sulfate (CE-SDS)

Purified proteins were analyzed by Capillary Electrophoresis Sodium Dodecyl Sulfate (CE-SDS) under non-reducing as well as reducing conditions on a CESI8000 instrument (AB Sciex) following the manufacturer's protocol from the IgG purity/heterogeneity kit. Before the measurement *via* pressure injection, the buffer was adjusted to 50 mM Tris pH 7.5, 50 mM NaCl.

Supplementary Figures

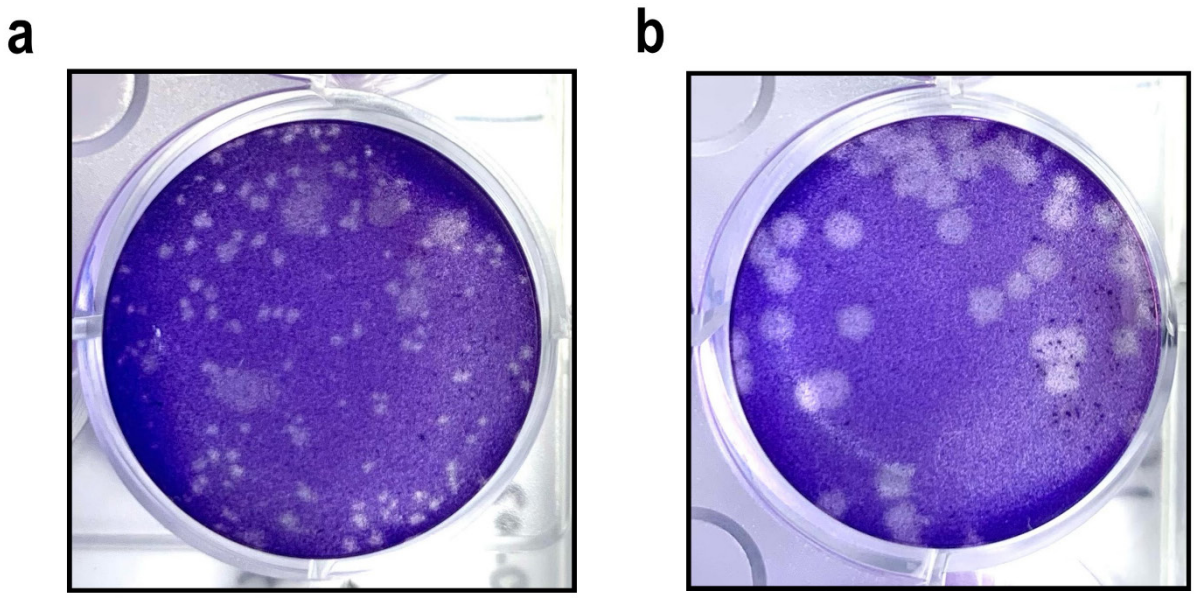

Supplementary Figure 1 ***Plaque appearance.*** *Viral plaques following infection of HepG2 cells with* ***a*** *SARS-CoV-2-Jan or* ***b*** *SARS-CoV-2-April.*

Supplementary Tables

Supplementary Table 1 Yield and purity of the ACE2-Fc constructs

Construct	Normalized Relative Yield*	HMWS (%) Analytical SEC	Purity CE-SDS non-reduced	Purity CE-SDS reduced
1	0.8	2.1	97.3	96.7
2	0.6	4.7	97.4	97.4
3	1.0	3.1	95.1	94.8
4	0.6	3.7	97.0	98.2
5	1.0	2.6	97.0	95.2
6	0.6	3.4	97.2	96.8
7	0.9	1.9	95.3	96.7
8	0.8	3.7	96.9	97.8

* Normalized against construct 5